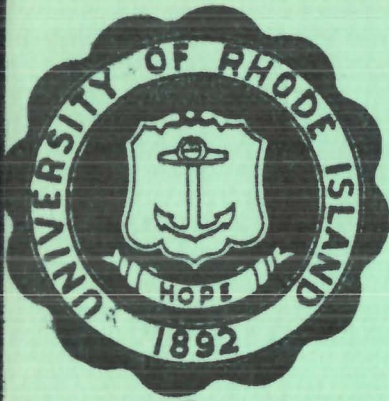




191607

JUNE 15, 1965

*DE 7*



DIVISION OF ENGINEERING RESEARCH AND DEVELOPMENT  
DEPARTMENT OF ELECTRICAL ENGINEERING

This document has been determined  
to fall under Distribution Statement  
per DODI 5230.24 dated 23 AUG 2012.

# Sea-State Observations With an Underwater Acoustic Signal

by  
L. O. JACOTIN

and  
R. F. HILL

Technical Report No. 11

Sponsor U.S. Navy  
Underwater Ordinance Station  
Contract No. N140(122)76682B  
Authority No. 0741807  
Project No. 42145

UNIVERSITY OF RHODE ISLAND  
KINGSTON, RHODE ISLAND

University of Rhode Island  
Division of Engineering Research and Development  
Electrical Engineering Department

Underwater Acoustics Technical Report No. 11

SEA-STATE OBSERVATIONS WITH  
AN UNDERWATER ACOUSTIC SIGNAL

By

Leonidas O. Jacotin

and

Richard F. Hill

Sponsor: U. S. Naval Underwater Ordnance Station

Date: June 15, 1965

## ABSTRACT

Experiments conducted in a model tank are concerned with reflection of an acoustic signal from the surface. The statistical distributions of the amplitude and phase of this reflected signal are considered. The statistical parameters describing the height and slope of the surface have been the object of recent researches. However, the relationship between the parameters associated with the reflected signal and the parameters of the surface is not well developed.

The purpose of this paper is to relate these two sets of parameters, or more specifically, the parameters of the reflected signal to the parameters of the waveheight of the surface. To achieve this purpose, an experiment is conducted consisting essentially of recording simultaneously an acoustic signal reflected from the surface and the output of a waveheight detector, and of analyzing each. This experiment confirms the fact that the received signals, for several different surface states obtained with a wind generator, are well approximated by a Rayleigh probability density function. The outputs of the waveheight indicator are Gaussian distributed with increasing maximum amplitude as the wind speed decreases.

Most significantly, a linear relationship between the ratio of the standard deviation  $\sigma_e$  to the root mean square value  $V_{rms}$  of the signal, and the standard deviation of the waveheights  $\sigma_w$  is obtained. This relationship can be expressed in the simple form  $\sigma_e = KV_{rms} \sigma_w$ . Such a result is quite satisfactory and indicates the possibility of a method for the observation of sea-state in which the only quantity observed will be an underwater acoustic signal reflected from the surface. In applications concerning the ocean, this method will have the advantage of being completely uncoupled from the surface itself.

## TABLE OF CONTENTS

	Page
CHAPTER 1: INTRODUCTION.....	1
1.1 History of Investigations.....	1
1.2 Brief Theoretical Description of the Problem .....	3
1.3 Plan of Attack .....	4
CHAPTER 2: DESCRIPTION OF EXPERIMENT .....	5
2.1 Model Tank .....	5
2.2 Water Wave Generation .....	5
2.3 Waveheight Indicator .....	5
2.4 Signal Generation, Transmission, Reception and Recording..	8
2.5 Analysis of the Experiment .....	9
CHAPTER 3: DATA ANALYSIS AND RESULTS .....	10
3.1 Probability Distribution and Probability Density Functions	10
3.2 Mean Value, Standard Deviation and Ergodic Theorem.....	14
3.3 Applications of Data Analysis Methods .....	18
3.4 Results .....	20
CHAPTER 4: THEORETICAL CONSIDERATIONS .....	23
4.1 Introduction .....	23
4.2 Analytical Model .....	23
4.3 Probability Density Functions .....	28
4.4 Investigations of the Final Result .....	32
CHAPTER 5: CONCLUSION .....	34

## INTRODUCTION

The surface of the ocean is of considerable interest to oceanographers, meteorologists, and, of course, all seafaring men. Techniques for observing the "sea-state", a measure of the average waveheight, are of increasing interest as the effect of the ocean surface on information-bearing underwater acoustic signals receives increasing attention. So far, the techniques available are not completely satisfactory due to limitations in size, location, or cost. In recent years, many important contributions have been made to the analysis of underwater acoustic reflection from the surface and the question may be asked whether or not it is possible to use these acquisitions for sea states observations and predictions. The investigation of such a possibility, its advantages and imperfections, constitute the purpose of this paper.

1-1. History of Investigations

As far as it is known, the first careful observation of ocean waves was initiated by Leonardo da Vinci<sup>13</sup> (1452-1519), and the first systematic mathematical study of wave motions appears to have been made by Sir Isaac Newton<sup>13</sup> (1642-1727). However, theory and experiments were quite uncorrelated. Observations were made whose results can be found in the publications of T. Stevenson<sup>13</sup> (1850), G. Schott<sup>13</sup> (1893) and V. Cornish<sup>2</sup> (1934). The theory received some developments with G. G. Stokes<sup>13</sup> (1847), F. Boussinesq<sup>13</sup> (1872), and Lord Rayleigh<sup>13</sup> (1876).

In 1925 H. Jeffrey<sup>15</sup> made an attempt to correlate theory and observations and H. U. Sverdrup and W. H. Munk<sup>18</sup> developed some empirical relationships making possible the forecast of wave height and period. More complete statistical descriptions of the sea surface was given later by M. S. Longuet-Higgins<sup>13</sup> (1946-48) and Willard Pierson<sup>16</sup>. In 1948 also,

L. N. Liebermann<sup>12</sup> obtained waveheight data by photographing, with a motion picture camera, the sea surface against a six foot scale. C. Eckart<sup>6</sup> in 1953 gave the first statistical theory of wave generation. In 1954, Cox and Munk<sup>3</sup> made measurements of the sea surface heights and slopes from photographs of the sun's glitter. In 1958 Longuet-Higgins<sup>14</sup> proposed a mathematical model of a random surface. In 1963 Gulin and Malishev<sup>7</sup> studied the statistical characteristics of the sea surface. D. Tetreault and R. F. Hill<sup>19</sup> recently utilized a capacitance probe for the observation of the waveheight statistics of a rough water surface in a model tank.

The other point of interest is the investigation of acoustic signals reflected from the sea surface. Among the best studies in this area, a few are selected here. In 1953, C. Eckart<sup>6</sup> presented a theory on the scattering of sound from the sea surface and showed experimentally that short wave radiations, like the sun's radiations, give much less information than long wave radiations like sound. In 1955, E. O. LaCasce and P. Tamarkin<sup>9</sup>, following the theories of Rayleigh, Eckart and Brekhovskikh, calculated the dependence on surface and radiation parameters, of the amplitudes of a reflected signal from a pressure-release surface, and compared these calculations with the results of their own experiment. Other experimental results due to D. C. Whitmarsh, E. Skudrzyk and R. F. Urik<sup>10</sup>, (1957) were given also on the scattering of sound by the sea surface. E. O. LaCasce<sup>8</sup> in 1958 presented a paper on scattering at angles near incidence. Measurements on amplitude fluctuation of surface reflected signals to deep hydrophones were taken by J. Beckerle<sup>1</sup> in 1962 and showed that the signal amplitude distribution can be described in terms of a Rayleigh distribution modified by adding a single contribution of random phase. R. M. Richter<sup>17</sup> presented in

1964 some measurements of ocean surface backscattering and the results confirmed that scattering strength is proportional to wind velocity and also to carrier frequency. In the same year, R. D'Antonio and R. F. Hill<sup>4</sup> studied the scattering in the specular direction of an acoustic signal reflected from a random surface in a model tank, and their results were in good agreement with actual measurements in the ocean. They also proposed a mathematical model to explain the results based on the assumption that received signal in the specular direction is the sum of individual rays coming from the horizontal facets in the sonified area.

### 1.2 Brief Theoretical Description of the Problem

The appearance of a wind generated water surface can be considered as a series of irregularly moving ridges and hollows gradually growing and shrinking with time. If the effect of spray rising into the air and air bubbles in the water is neglected, this surface can be represented by a single valued function of the coordinates  $x$ ,  $y$  and time  $t$ , i.e.  $\eta(x,y,t)$ . The air motions above the surface and the water motions below it must satisfy the nonlinear equations for fluid motions subjected to nonlinear boundary conditions at this surface. These equations have not yet been solved exactly. However, if attention is concentrated on measurements at a fixed point as a function of time, techniques of varying degrees of precision have been developed to measure  $\eta(t)$ . The usual procedure consists of recording the output of a device over a period of time and analyzing the record. The experiment may be conducted in the open sea, or in a model tank. One of the problems is how to analyze these records. When the assumption is made that they are samples of quasi-stationary random process that is approximately Gaussian, techniques of analyses can be found. But when the records are decidedly non-Gaussian in character, techniques remain to be developed. This paper is principally based upon this assumption of a quasi-stationary random Gaussian process and such an assumption has

has appeared to be quite logical<sup>4</sup>.

Several devices can be used to obtain a record of a wind driven surface. Visual observations, photography, and variable capacity probes are among the most common. They can be satisfactory in some respects but their utility is often limited. Lack of time to perform many records and to analyze them, impossibility to reach the water surface in other applications, and even cost of operations can be prohibitive, in many instances. It is believed that a more reliable method can be proposed using the fact that an underwater acoustic signal after reflection from a random surface bears information about the surface itself. Therefore, the problem to be investigated is the correlation of the time varying waveheight of wind generated surfaces with signals reflected from such surfaces.

### 1-3. Plan of Attack

In dealing with this problem, the following procedure is followed:

(a) an acoustic beam is reflected and received almost normal to the calm position of the surface; (b) the signal received is amplitude demodulated and recorded along with the output of an instantaneous waveheight detector; (c) records taken for various surface states are analyzed and compared; (d) finally, a mathematical model is proposed to explain the results.

## 2.

## DESCRIPTION OF EXPERIMENT

2-1. Model Tank

The experiment is conducted in a steel tank, 12 feet long, 4 feet wide and 4 feet high, filled with fresh water. An absorbent lining is placed at the bottom of the tank to eliminate interference from multiple reflections.

The two transducers used are 2 inches in diameter and situated 5 inches from each other. With their faces making an angle of 85 degrees with the vertical, the incident and reflected beams are almost normal to the calm surface of the water in the tank. A transducer positioning control system serves to position the pair at a particular depth and place in the tank. This location is the same for all parts of the experiment.

2-2. Water Wave Generation

Water waves that model the ocean surface are obtained with four 20 inch, three-speed fans mounted in two stacks of two on a wooden frame. Waves can be generated by varying the distance from the water surface to the faces of the fans, by varying the angle between water surface and faces, and by changing the speed of the fans. In this application, the last method is preferred because a larger area over which the waves have spatial stationarity exists when the faces of the fans are parallel with the calm surface of the water. Ten different states of the water are considered in this experiment and are obtained with both fans in each horizontal pair operating at the same speed.

The tank, the servosystem and the fan arrangement can be seen in Fig. 1.

2-3. Waveheight Indicator

The waveheight indicator is an active device consisting essentially of a square wave generator and a resistor in series with a variable capacitor.

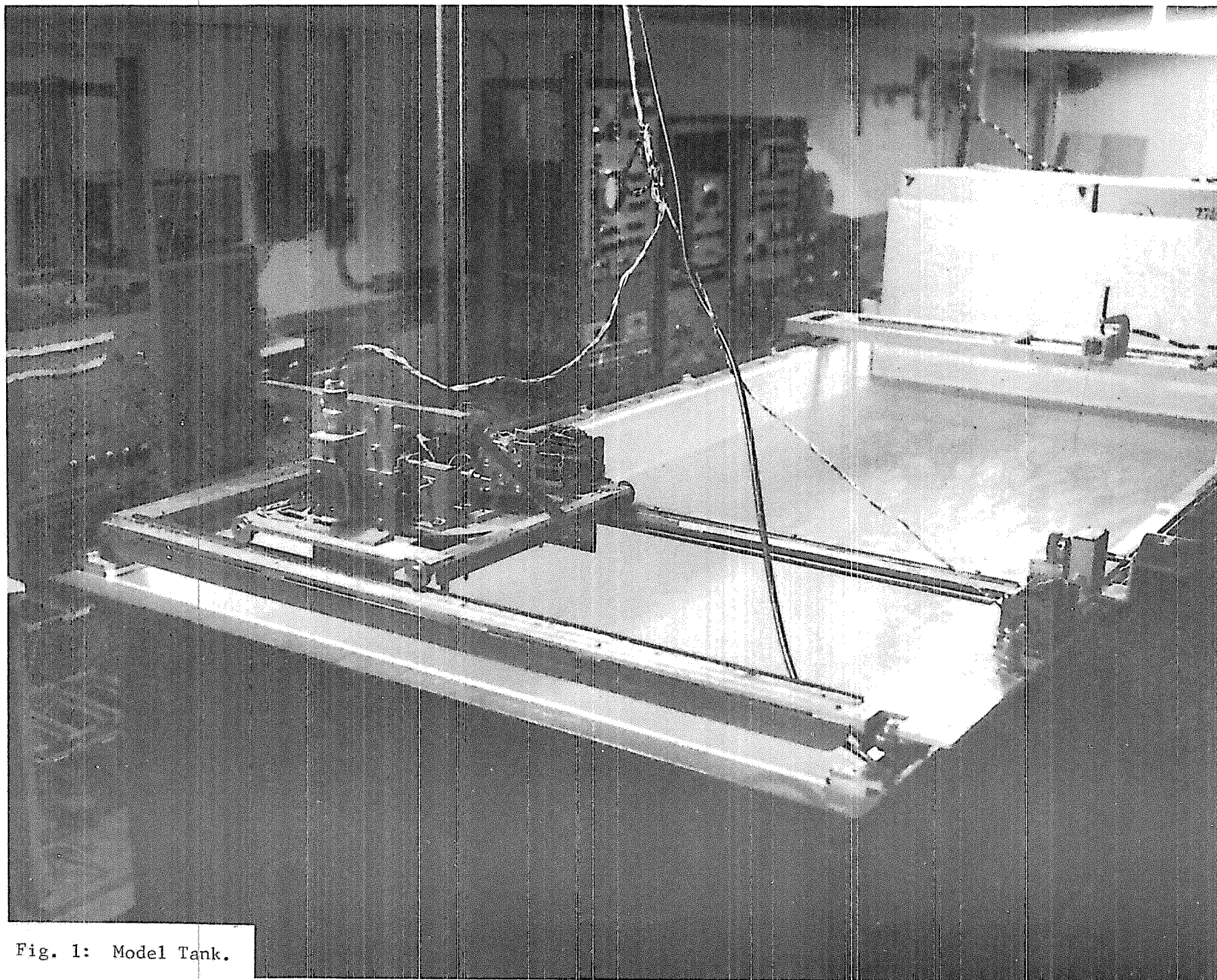
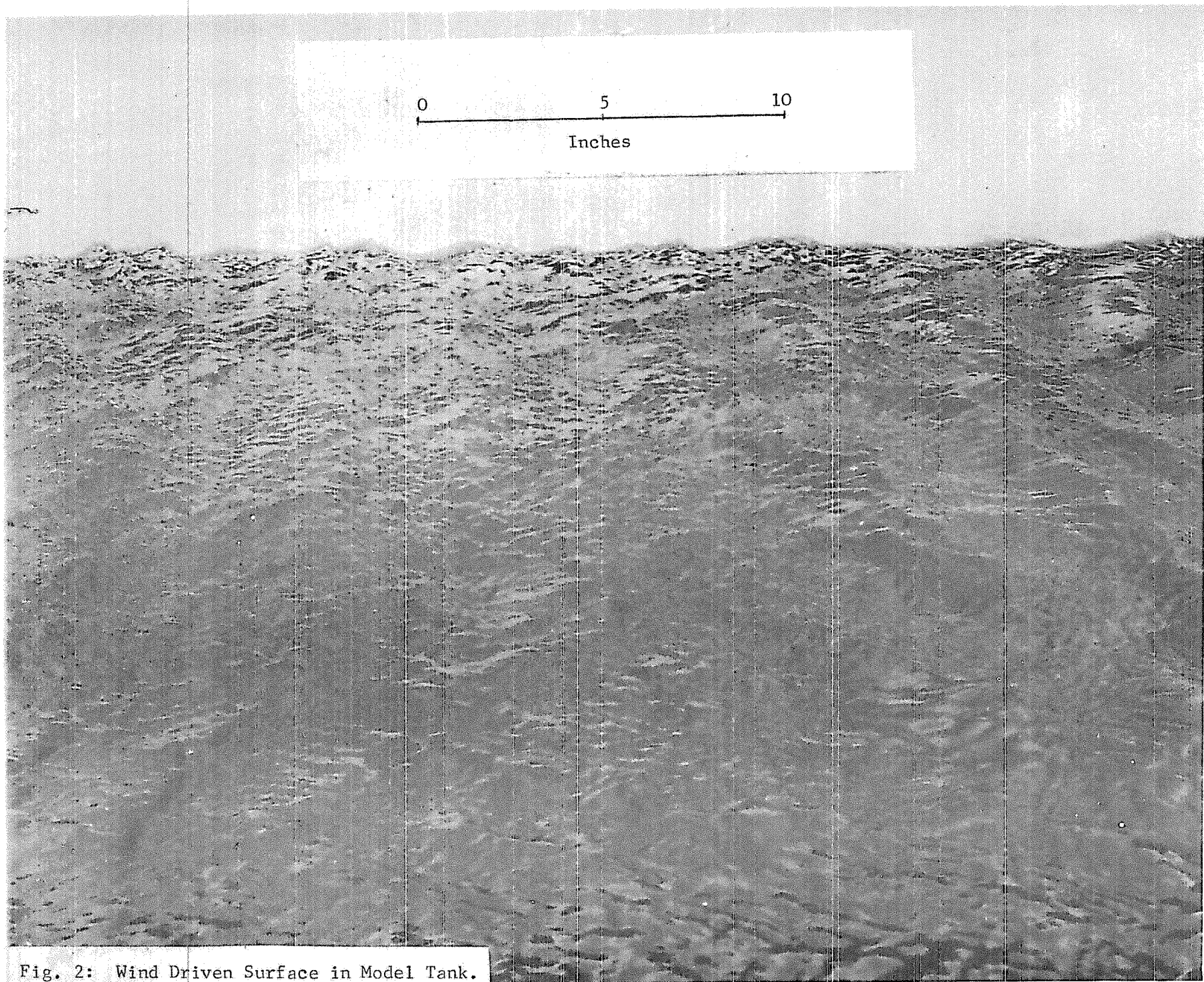


Fig. 1: Model Tank.



One plate of this capacitor, called the probe, is a piece of Formvar No. 14 copper wire coated with a thin dielectric enamel; the other plate is the tank itself. When a portion of the probe is in the water, the capacitance is proportional to the height of the water around the probe. The frequency of the square wave generator is chosen so that the voltage across the resistor is proportional, at any instant of time, to the capacitance, therefore giving a measurement of waveheight. The device, as used in the experiment, has a linearity of better than 2 percent over its useful range. The probe can be seen in Fig. 1 between the fans and the servo mechanism. A complete description of the waveheight detector system is given in reference 4.

Figure 2 is a typical picture of the generated surface. The scale shown can be converted in acoustic wavelengths taking 1/25 inch for one acoustic wavelength. Also, it can be noted that the water waves are about two to three inches in length.

#### 2-4. Signal Generation, Transmission, Reception, and Recording

A Hewlett-Packard Model 606A signal generator is used to generate a continuous sine wave at a frequency of 815 kc, the resonant frequency of the transducers. The signal is amplified by a General Radio, Type 1233-A power amplifier and applied to the transmitting transducer. After reflection from the surface, the signal is picked up by the receiving transducer. Transmitter and receiver are made of barium titanate slabs, 2 inches in diameter supplied by Gulton Industries. The beam patterns are almost identical and show a beam width of approximately 3 degrees between the half power points when operated at resonance (see Fig. 3). The transducers are 30 inches below the water surface. The received signal is amplitude demodulated, amplified, and recorded on one FM channel of a seven channel Sanborn magnetic tape recorder.

A second FM channel is used for simultaneous recording of the output of the waveheight detector. An overall picture of the process involved is given by the flow diagram of Fig. 4.

#### 2-5. Analysis of the Experiment

The object of this research being sea-state observation, the ideal situation is one in which a single ray sonifies a single point on the surface. The travel time between transmitter and receiver would then be a simple function of the height of the point. In actuality, a relatively large area of the surface is sonified. In this experiment, the sonified area, defined as the area within the half power circle, has a diameter of 1.5 inches. Such an area includes many horizontal facets as can be seen in Fig. 2. Each ray impinging on a horizontal facet will return to the receiver. The received signal will be then the summation of many such rays with different travel times. To take each small contribution into account, a statistical study of the reflected signal is in order.

Signals are recorded for different water surfaces, which model different sea-states, and at least 15 minute intervals are taken between consecutive records to assume reasonable stationarity and each record is ten minutes long.

## 3.

## DATA ANALYSIS AND RESULTS

3-1. Probability Distribution and Probability Density Functions

In the analysis of the data, the first point achieved is the determination of the probability distribution function defined as:

$$P(x \geq X) = \lim_{T \rightarrow \infty} \frac{T_x}{T} \quad (3-1)$$

where  $T$  is an interval of time chosen large enough so that the signal  $x$  being analyzed can be considered as stationary; and  $T_x$  is the amount of time, during the interval  $T$ , for which the signal is greater than  $X$ .

Then the probability density function can be obtained as:

$$p(x) = - \frac{dP(x \geq X)}{dx} \quad (3-2)$$

The minus sign takes into account the fact that the probability distribution function defined by (3-1) is unity minus the conventional probability distribution function, that is, if  $P'(x \leq X)$  denotes the usually defined probability distribution function, then:

$$P'(x \leq X) = 1 - P(x \geq X) \quad (3-3)$$

$$\text{and } p(x) = \frac{dP'(x \leq X)}{dx} = - \frac{dP(x \geq X)}{dx} \quad (3-4)$$

For the purpose of analysis,  $X$  is a reference magnitude or, for a voltage signal, a threshold voltage  $E_0$ , and  $x$  the instantaneous value  $E_s$  of the signal.

A circuit designed to compare  $E_s$  to  $E_0$  is given in Fig. 5. In this diagram, the input current to the amplifier is

$$i = \frac{E_s}{R_1} + \frac{E_{\text{ref}}}{R_2} \quad (3-5)$$

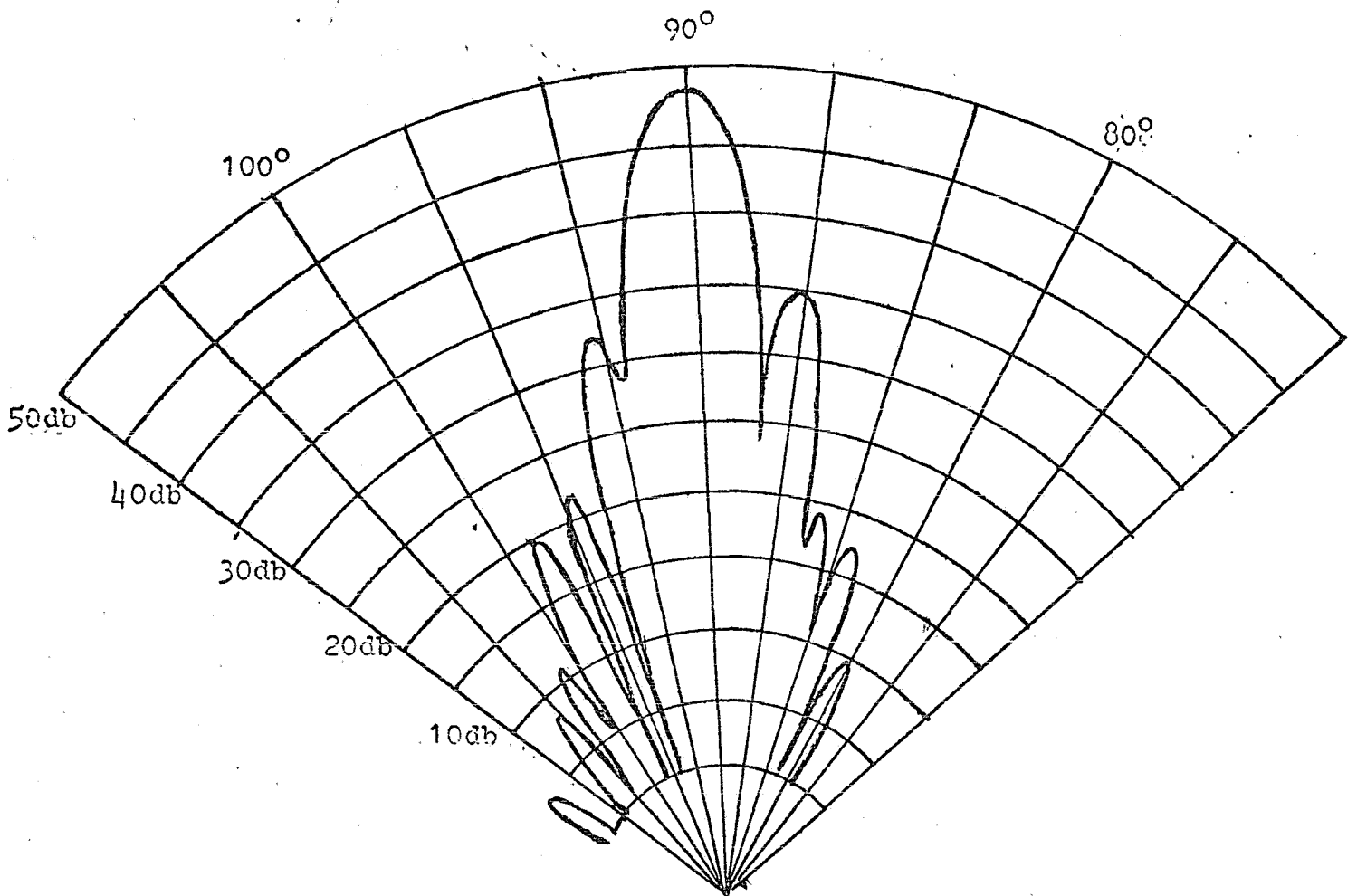


Fig. 3 Transducer Directivity Pattern at 815 kcs

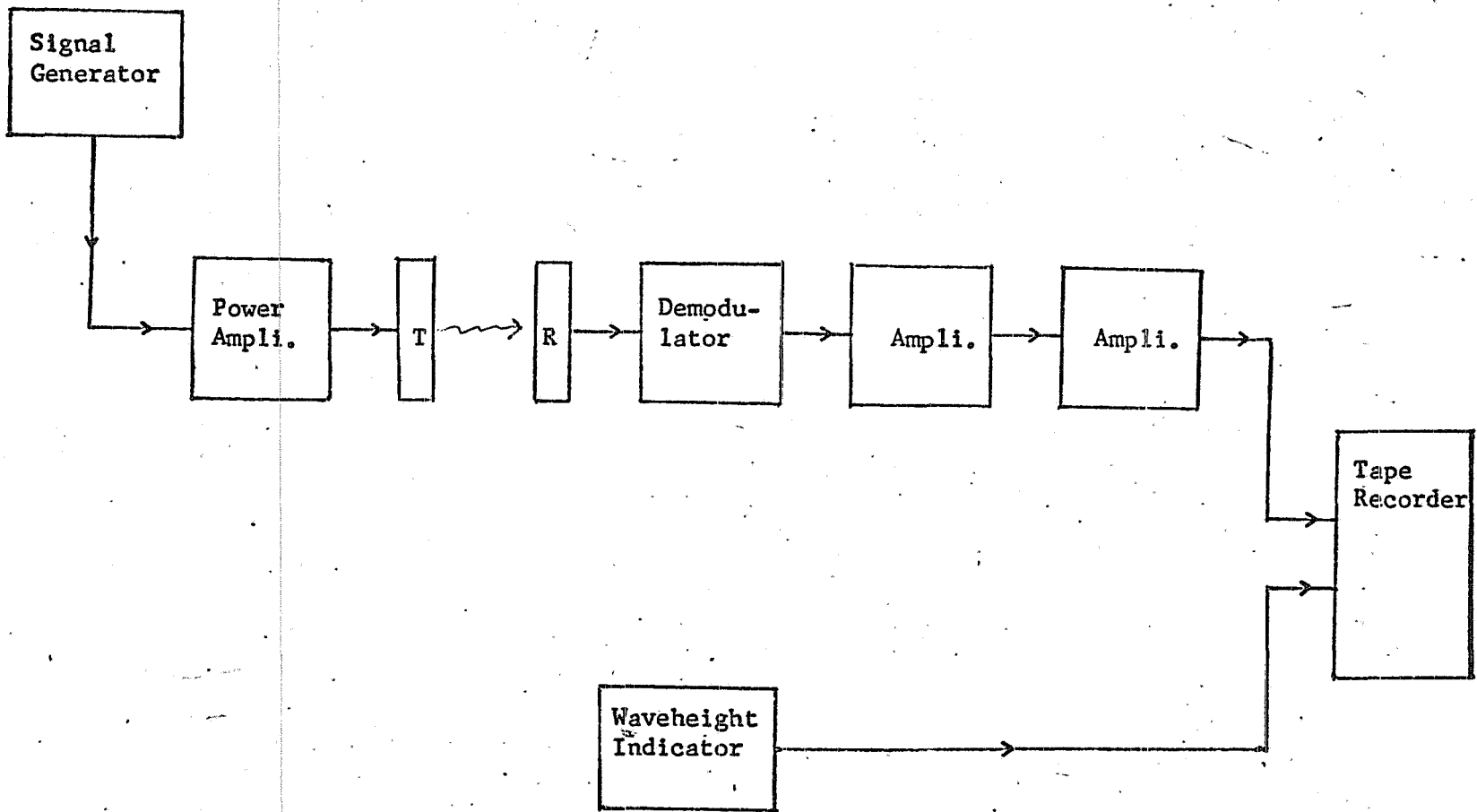


Fig. 4 Flow Diagram of Experiment

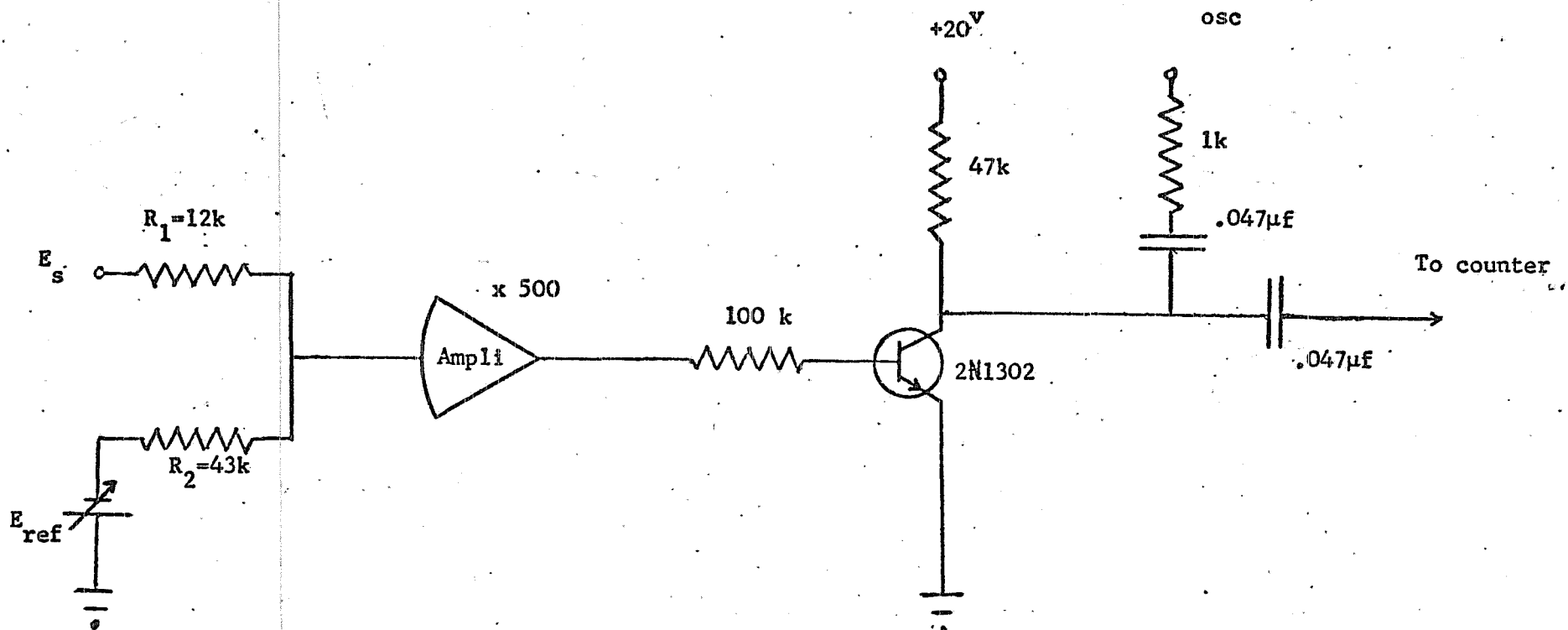


Fig. 5 Threshold Detector

When the signal passes through the value X

$$E_s = E_o = - \frac{R_1}{R_2} E_{ref} \quad (3-6)$$

and the direction of the current changes. With the amplifier working into saturation, its output will be:

$$+ \text{ saturation whenever } E_s \geq - \frac{R_1}{R_2} E_{ref} \text{ or } E_s \geq E_o \quad (3-7a)$$

$$- \text{ saturation whenever } E_s < - \frac{R_1}{R_2} E_{ref} \text{ or } E_s < E_o \quad (3-7b)$$

The output of this amplifier is used to trigger a gate on the output of a 20 kc oscillator. An electronic counter is used to count the number of cycles passed by the gate during a one minute sample period and thus determine the amount of time that the signal is above the reference level, Figs. 6 and 7).

### 3-2. Mean Value, Standard Deviation, and Ergodic Theorem

The mean value of a random variable  $x_t$  with probability density function  $p(x_t)$  is given by:

$$m_x = \int_{-\infty}^{+\infty} x_t p(x_t) dx_t \quad (3-8)$$

$x_t$  as above refers to the possible values which can be assumed at the time instant  $t$  by the sample signal  $x(t)$ . The random process with which we are dealing is assumed to be stationary, meaning that  $p(x_t)$  is the same regardless of the time  $t$ , or  $m_x$  does not change with time. Furthermore, a time average for  $x(t)$  can be defined as

$$\langle x(t) \rangle = \lim_{T \rightarrow \infty} \frac{1}{2T} \int_{-T}^T x(t) dt \quad (3-9)$$

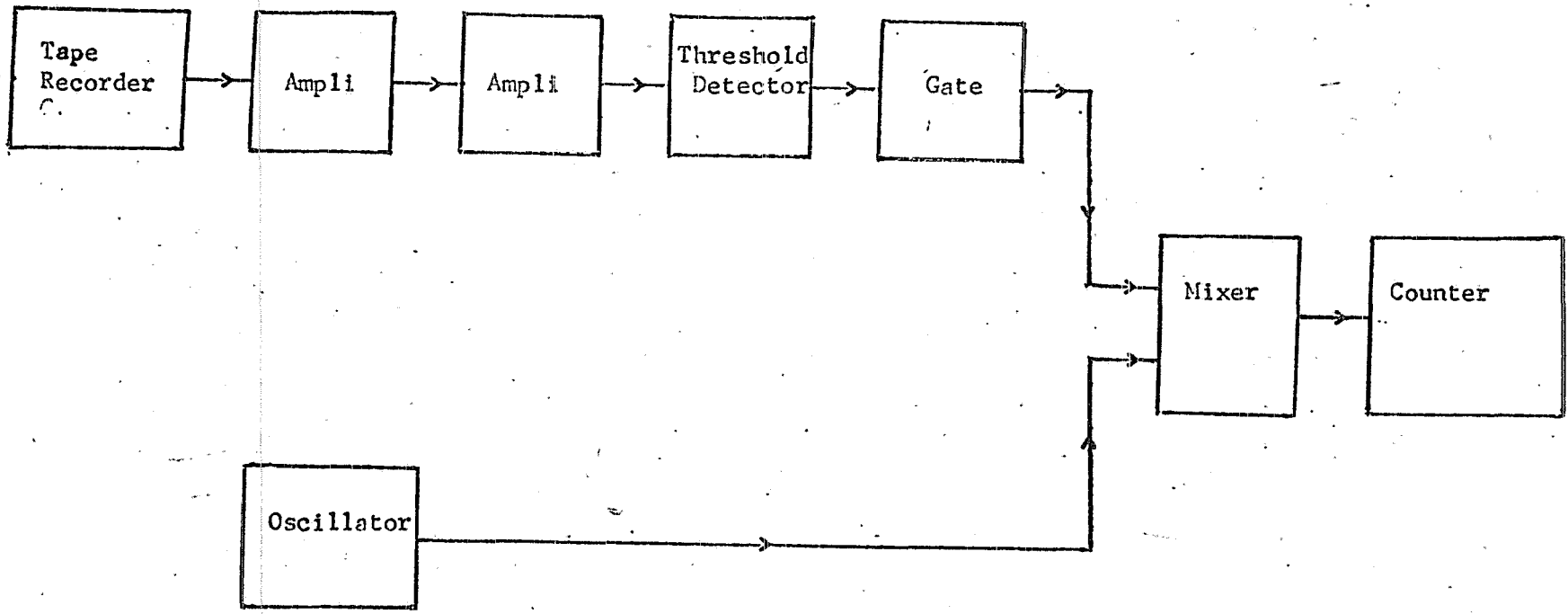


Fig. 6 Flow Diagram of Analyser

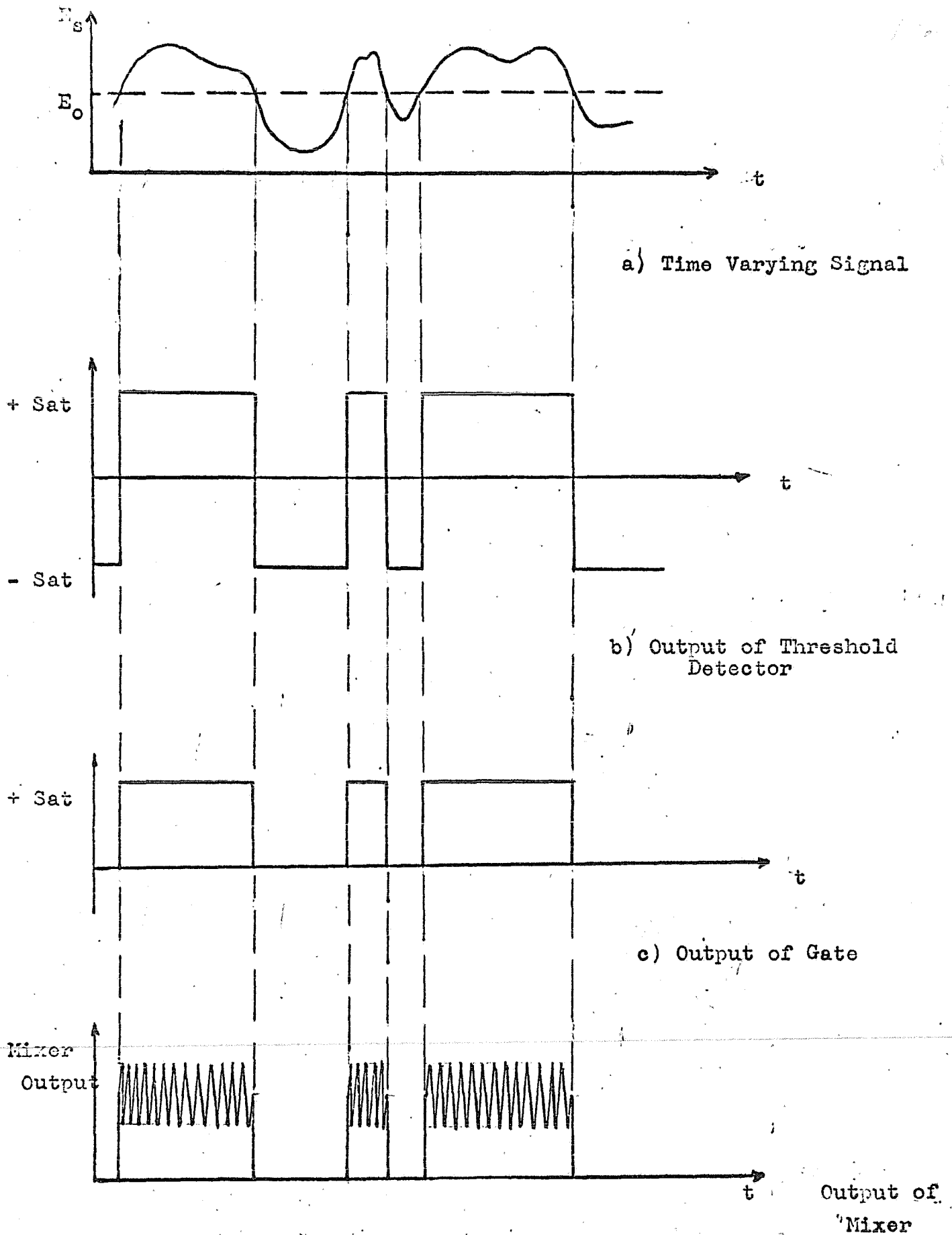


Fig. 7 Outputs of Various Positions of Analyser

The ergodic theorem<sup>5</sup> guarantees that the limit of  $\langle x(t) \rangle$  in the case of a stationary random process exists for every sample function except for a set with probability zero, and under a certain condition called ergodicity, this limit is equal with probability one to the constant statistical average,  $m_x$ . Thus, under the valid ergodic hypothesis,

$$m_x = \langle x(t) \rangle \quad (3-10)$$

For purpose of calculation,  $p(x_t)$  in equation (3-8) is sampled at different points and  $m_x$  found as:

$$m_x = \sum_{i=1}^N x_i p(x_i) \Delta x_i \quad (3-11)$$

The mean was also observed by averaging the signal in the time domain for one minute with an analog computer (Electronics Associates TR-48). The computer diagram is given by Fig. 8. Equation (3-8) has been used to ascertain the results.

The other quantity of interest is the variance:

$$\sigma_x^2 = \int_{-\infty}^{+\infty} (x_t - m_x)^2 p(x_t) dx_t \quad (3-12)$$

This integral is evaluated as:

$$\sigma_x^2 = \sum_{i=1}^N (x_i - m_x)^2 p(x_i) \Delta x_i \quad (3-13)$$

The standard deviation is obtained as  $\sigma_x$ .

From equation (3-11) the variance can also be written as:

$$\sigma_x^2 = E(x_t^2) - m_x^2 \quad (3-14)$$

where:

$$E(x_t^2) \equiv \int_{-\infty}^{+\infty} x_t^2 p(x_t) dx_t \quad (3-15)$$

Applying the ergodic hypothesis

$$E(x_t^2) = \lim_{T \rightarrow \infty} \frac{1}{2T} \int_{-T}^T x^2(t) dt \quad (3-16)$$

which is found using the analog computer programmed as shown in Fig. 9.

Finally, the variance is obtained from the two analog computer results as:

$$\sigma_x^2 = E [x_t^2] - [\langle x(t) \rangle]^2 \quad (3-17)$$

### 3-3. Application of Data Analysis Methods

The recorded signals are analyzed utilizing the above equations.

First, the waveheight and envelope probability density functions are determined utilizing equation (3-2). The variances are obtained from the time domain expression given by equations (3-16) and (3-17). The time domain analysis is used since this yields a great saving in time. The use of equation (3-13) would require a complex programming of a digital computer. Finally, the ratio  $\frac{\sigma_e}{V_{rms}}$  has been computed and compared to  $\sigma_w$ ; where  $\sigma_e$ ,  $\sigma_w$  are the standard deviations of the envelope and waveheight output respectively, and  $V_{rms}$  the root mean square value of the received acoustic signal. Since the acoustic signal is composed of a constant average  $m_e$  and a time varying part  $x_e(t)$ , its mean square value can be obtained as:

$$V_{rms}^2 = \lim_{T \rightarrow \infty} \frac{1}{2T} \int_{-T}^T [m_e + x_e(t)]^2 dt \quad (3-18)$$

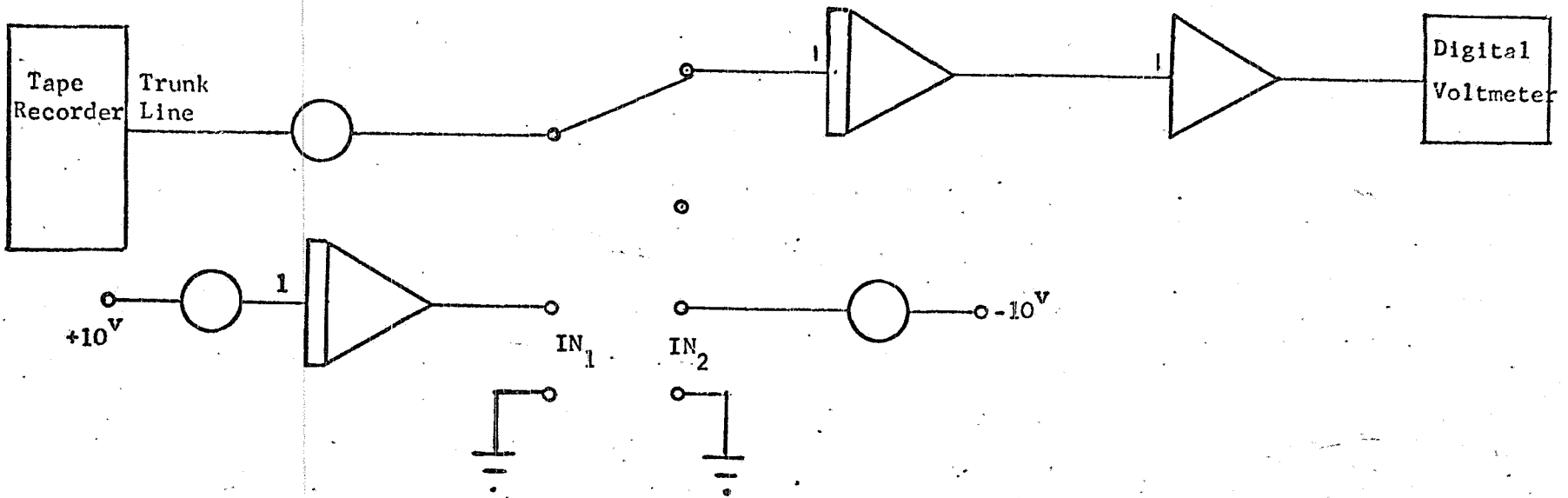


Fig. 8 Analog Computer Diagram for Determination of  $\langle x(t) \rangle$

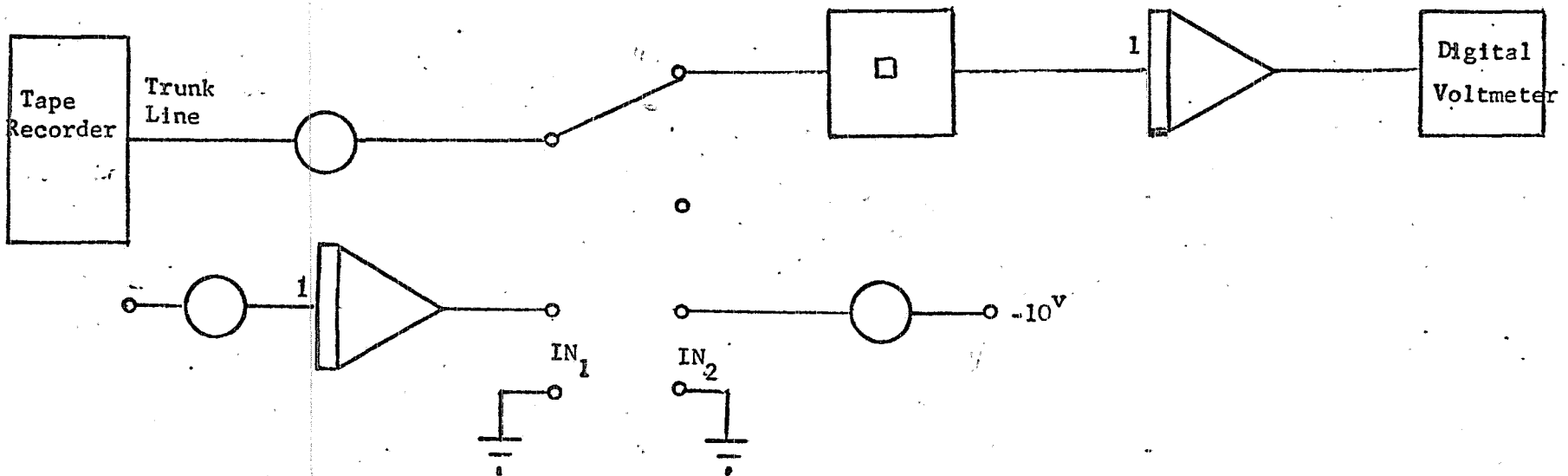


Fig. 9 Analog Computer Diagram for determination of  $\langle x^2(t) \rangle$

or

$$V_{\text{rms}}^2 = m_e^2 + 2m_e \lim_{T \rightarrow \infty} \frac{1}{2T} \int_{-T}^T x_e(t) dt + \lim_{T \rightarrow \infty} \frac{1}{2T} \int_{-T}^T x_e^2(t) dt \quad (3-19)$$

Noting that  $x_e(t)$  has no d-c component:

$$\lim_{T \rightarrow \infty} \frac{1}{2T} \int_{-T}^T x_e(t) dt = 0 \quad (3-20)$$

and that:

$$\lim_{T \rightarrow \infty} \frac{1}{2T} \int_{-T}^T x_e^2(t) dt = \sigma_e^2 \quad (3-21)$$

equation (3-19) can be written as:

$$V_{\text{rms}}^2 = m_e^2 + \sigma_e^2 \quad (3-22)$$

or

$$V_{\text{rms}} = \left[ m_e^2 + \sigma_e^2 \right]^{1/2} \quad (3-23)$$

Then  $\frac{\sigma_e}{V_{\text{rms}}}$  is determined:

$$\frac{\sigma_e}{V_{\text{rms}}} = \frac{\sigma_e}{\sigma_e^2 + m_e^2}^{1/2} \quad (3-24)$$

### 3-4. Results

Figure 10 shows probability density functions of the envelope of the received signal. They follow in general the form of a Rayleigh distribution, with a maximum amplitude shifting to the right as the speed of the wind decreases. Such distributions are not unexpected and have been reported in the literature<sup>4</sup>.

Figure 11 shows some of the probability density functions of the output of the waveheight detector. These curves are Gaussian, with an increasing

maximum amplitude for decreasing windspeed. The Gaussian distribution has been reported<sup>4,17</sup>, and the increasing maximum amplitude is due to the small waveheights which become dominant as the windspeed is decreased.

Figure 12 is the presentation of the final results of this work.

$\frac{\sigma_e}{V_{rms}}$  has been plotted against  $\sigma_w$ , and the different points obtained have suggested a straight line for a final curve. It seems, therefore, that  $\frac{\sigma_e}{V_{rms}}$  is linearly dependent upon  $\sigma_w$ . The explanation that is proposed here for this result is quite simple. As  $\sigma_w$  increases with windspeed, the tendency of  $\sigma_e$  is to increase first and then to decrease in absolute magnitude; however, the envelope of the received signal becomes more and more distorted and the energy is reflected more uniformly through all angles of reflection and thus a smaller amount returned in the normal direction. It seems apparent that  $V_{rms}$ , which measures the reflected energy, decreases faster than  $\sigma_e$ , or better the magnitude of the envelope variation increases relative to the signal strength. Then  $\frac{\sigma_e}{V_{rms}}$  increases with  $\sigma_w$ . Other methods of presentation of the final results have been studied, but this one is preferred since it yields to a much simpler expression.

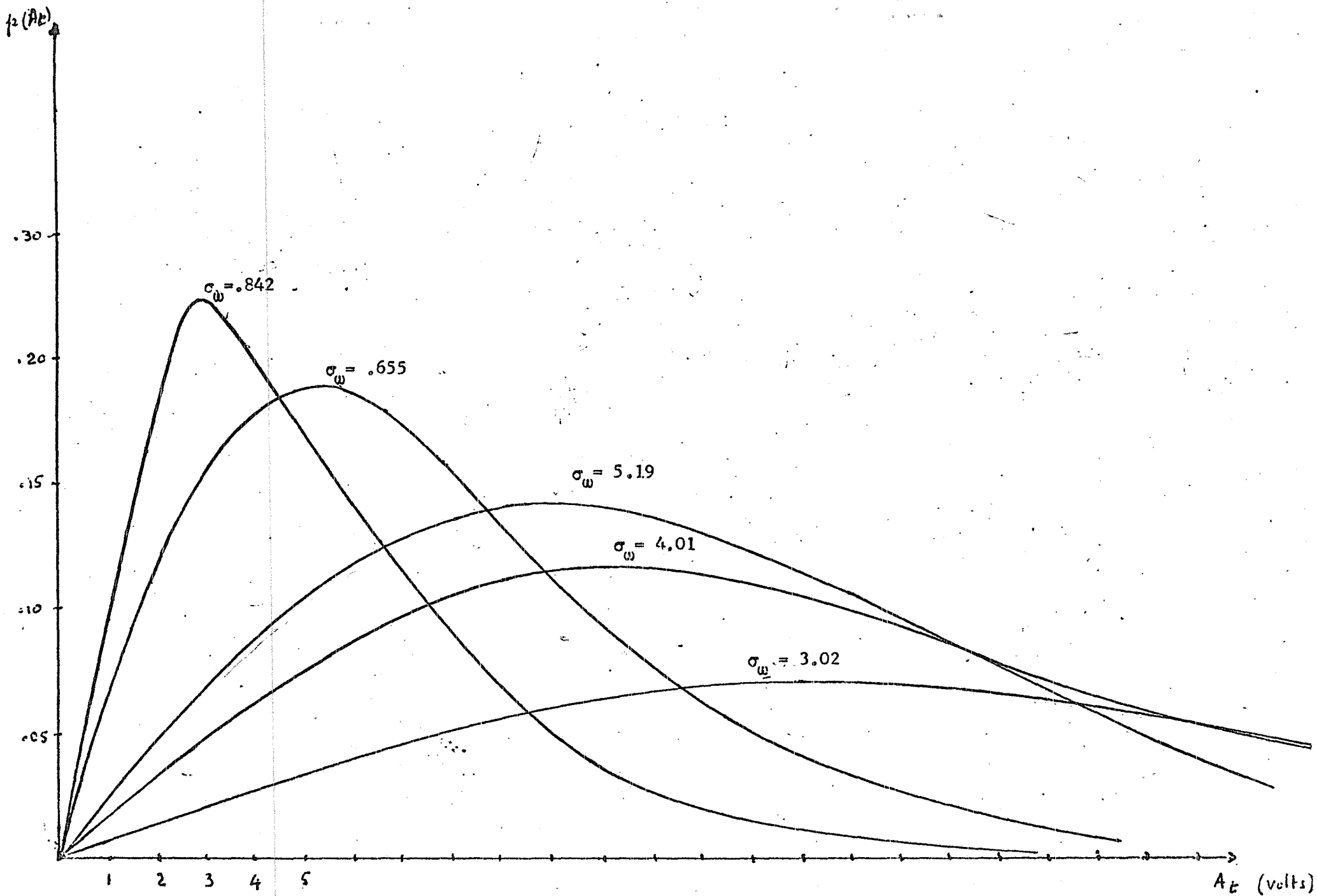


Fig. 10 Probability Density Curves of Envelope of Received Signal

## 4.

## THEORETICAL CONSIDERATIONS

4-1. Introduction

This chapter is a discussion of the theories involved in this work. The probability density function of the amplitude of the received signal is derived and compared with the probability density of the waveheight indicator and an attempt is made to explain the final results obtained. Figure 13 is a simplified diagram of the experiment conducted in the steel tank and shows the relative positions of the transmitter, receiver, and waveheight indicator.

The derivations that follow are primarily based on ray theory, and the usual conditions are satisfied, namely the change in curvature of a wavefront along a ray is negligible in terms of wavelength, the dimensions of the source and receiver are large compared to a wavelength, and the signal attenuation is low.

4-2. Analytical Model

Figure 17 is a magnified version of Figure 16. The reference axes are the vertical and a horizontal axis referring to the calm position of the surface. In the reflection of the incident beam, only the rays reflected in the specular direction are received by the second transducer. The path of a ray such as TAR is shown in Fig. 17, and the reference ray is taken as TBR'. The interest is here in the difference in path length of TAR and TBR', which is according to the figure:

$$\overline{\Delta d} = \overline{BA} + \overline{CB} \quad (4-1)$$

But  $\overline{CB} = \overline{BA} \cos 2\alpha$  (4-2)

And  $\overline{\Delta d} = \overline{BA} (1 + \cos 2\alpha)$  (4-3)

Making the trigonometric substitution

$$1 + \cos 2\alpha = 2 \cos^2 \alpha \quad (4-4)$$

4-3 becomes

$$\overline{\Delta d} = 2BA \cos^2 \alpha \quad (4-5)$$

Also

$$\overline{BA} = \frac{\overline{HA}}{\cos \alpha} \quad (4-6)$$

The expression for the path difference becomes

$$\overline{\Delta d} = 2\overline{HA} \cos \alpha \quad (4-7)$$

Where  $\alpha$  is the incident angle, and  $HA = h(t)$  is the variable height of the point A.

In this particular application  $\alpha$  is very small and  $\cos \alpha \cong 1$  and, (4-7) can be therefore written in the final form:

$$\overline{\Delta d} \cong 2h(t) \quad (4-8)$$

Introducing the wave number  $k$ , the phase difference between TAR and the reference ray can be obtained as:

$$\phi(t) = 2kh(t) \quad (4-9)$$

The received signal at an instant of time will be composed of many rays with different travel paths and when the transmitted signal is of the form

$$x_t = A_T \cos \omega_c t \quad (4-10)$$

each reflected ray will be of the form  $A_n \cos \left[ \omega_c t + \phi_n(t) \right]$ , where  $A_n$  is the amplitude of the ray and  $\phi_n(t)$  is its phase:

$$\phi_n(t) = 2kh_n(t) \quad (4-11)$$

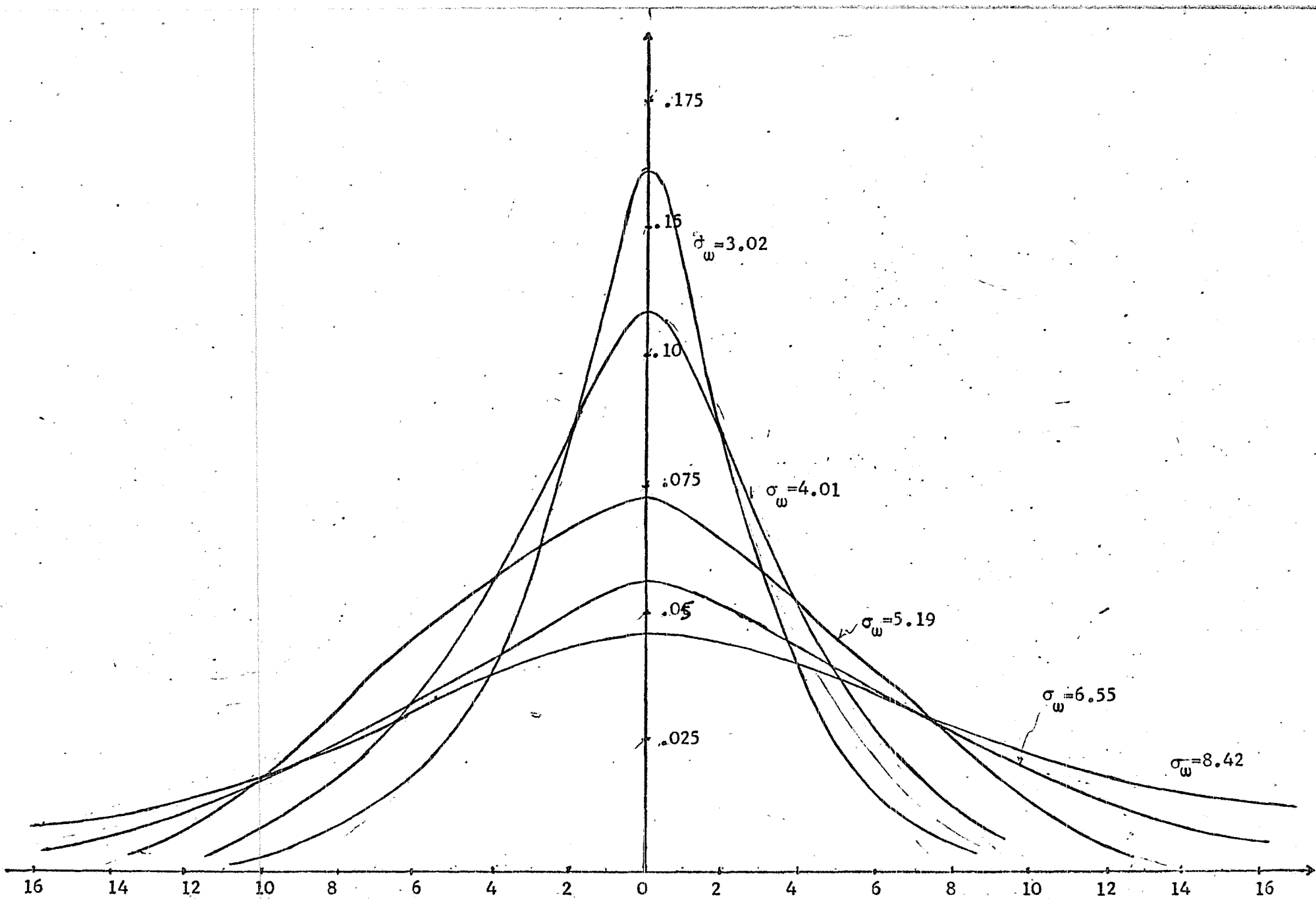


Fig. 11 Probability Density Curves of Waveheights

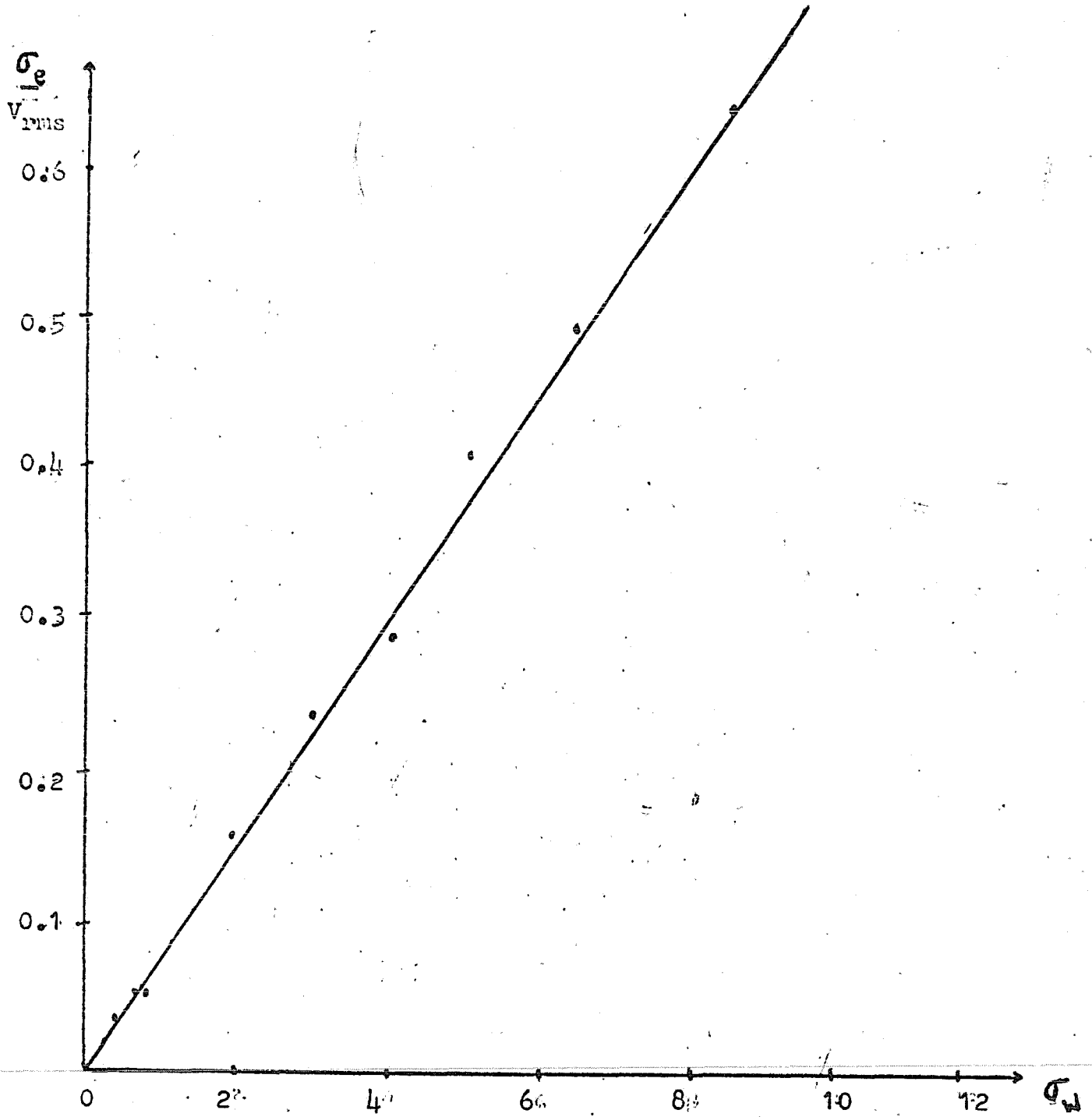


Fig. 12 Experimental Results and Straight Line Approximation

Fig. 13  
Simplified Diagram of  
Experiment

T - transmitter  
R - receiver.  
W - waveheight indicator

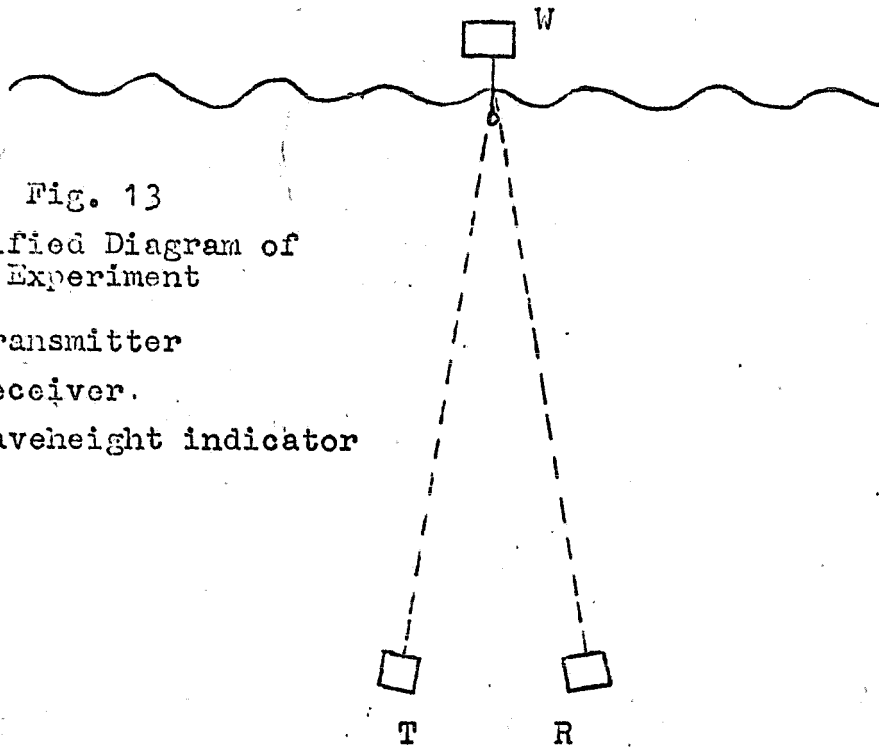
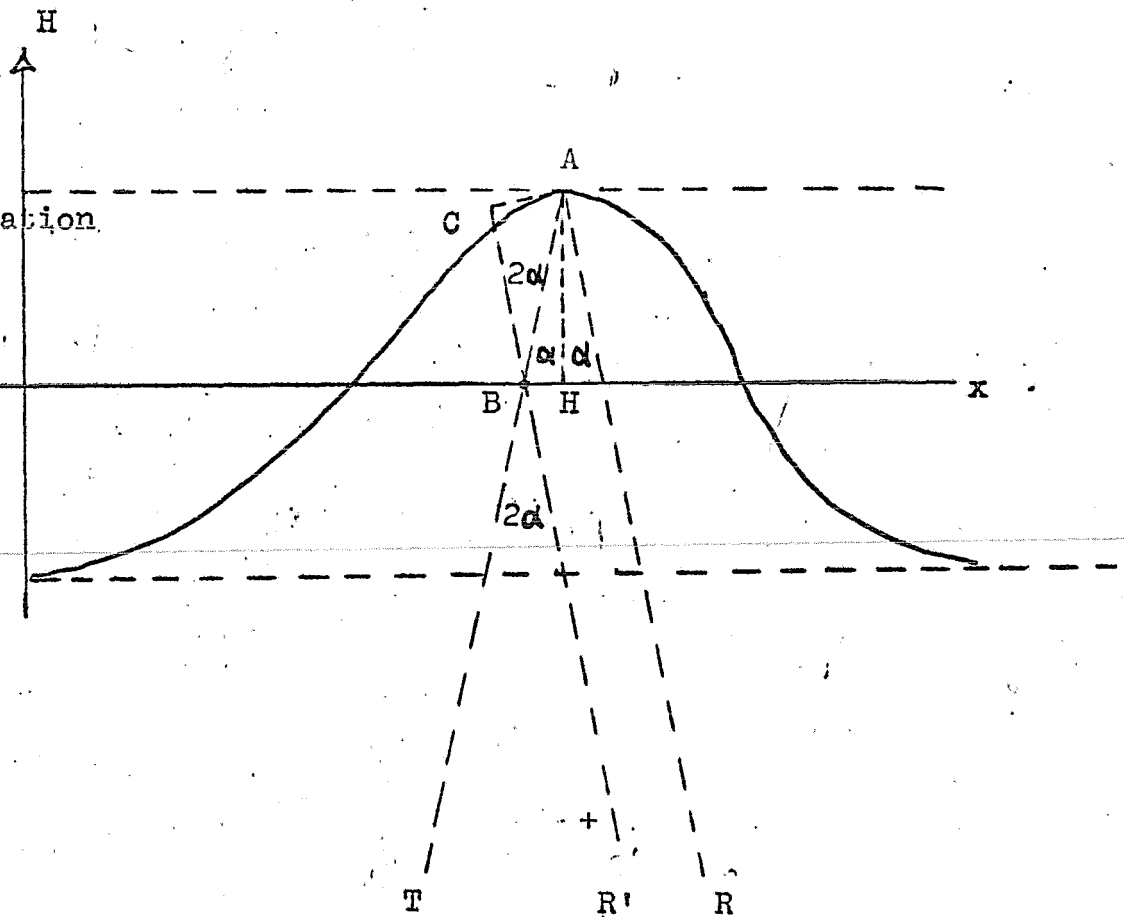


Fig. 14  
Diagram for calculation  
of difference  
in path length  
between two rays



The received signal will be then:

$$x_r = \sum_{n=1}^N A_n \text{Cos}[\omega_c t + \phi_n(t)] \quad (4-12)$$

The resultant of this summation will be:

$$x_r = A(t) \text{Cos}[\omega_c t + \phi(t)] \quad (4-13)$$

where  $A(t)$  and  $\phi(t)$  are random variables.

#### 4-3. Probability Density Functions

At this point, we want the probability density functions of the amplitude and phase of the received signal. From what has been said in the previous chapter, one may expect the result of this derivation to be a Rayleigh density function for the amplitude and a phase evenly distributed in the range 0 to  $2\pi$  since the receiver cannot distinguish between rays separated by  $2\pi$  or  $2k\pi$ ,  $K=0, 1, 2, 3$ .

A few assumptions largely satisfied in practice are necessary. The envelope  $A(t)$  and the phase  $\phi(t)$  are small compared to the variations of the transmitted signal.

Since the record of the signal was made for a finite amount of time, it is convenient to represent the received signal in an interval of time  $[0, t]$  by the Fourier Series:

$$x_r(t) = \sum_{n=1}^{\infty} [x_{cn} \text{Cos } n\omega_o t + x_{sn} \text{sin } n\omega_o t] \quad (4-14)$$

with

$$\omega_o = \frac{2\pi}{T} \quad (4-15a)$$

and

$$x_{cn} = \frac{2}{T} \int_0^T x_r(t) \text{Cos } n\omega_o t dt \quad (4-15b)$$

$$x_{sn} = \frac{2}{T} \int_0^T x_r(t) \sin n\omega_0 t \, dt \quad (4-15c)$$

It can be shown that  $x_{cn}$  and  $x_{sn}$  are also Gaussian random variables which become uncorrelated as the expansion interval increases without limit.

The carrier frequency is introduced by writing equation (4-14) in the following form:

$$x_r(t) = \sum_{n=1}^{\infty} x_{cn} \cos[(n\omega_0 - \omega_c)t + \omega_c t] + x_{sn} \sin[(n\omega_0 - \omega_c)t + \omega_c t] \quad (4-16)$$

Defining:

$$x_c(t) = \sum_{n=1}^{\infty} [x_{cn} \cos(n\omega_0 - \omega_c)t + x_{sn} \sin(n\omega_0 - \omega_c)t] \quad (4-17a)$$

$$x_s(t) = \sum_{n=1}^{\infty} [x_{cn} \sin(n\omega_0 - \omega_c)t - x_{sn} \cos(n\omega_0 - \omega_c)t]$$

then:

$$x_r(t) = x_c(t) \cos \omega_c t - x_s(t) \sin \omega_c t \quad (4-18)$$

For comparison, equation (4-13) is rewritten:

$$x_r(t) = A(t) \cos[\omega_c t + \phi(t)] \quad (4-13)$$

or:

$$x_r(t) = A(t) \cos \phi(t) \cos \omega_c t - A(t) \sin \phi(t) \sin \omega_c t \quad (4-19)$$

Then from (4-18) and (4-19)

$$x_c(t) = A(t) \cos \phi(t) \quad (4-20a)$$

$$x_s(t) = A(t) \sin \phi(t) \quad (4-20b)$$

and

$$A(t) = \left[ x_c^2(t) + x_s^2(t) \right]^{1/2} \quad (4-21a)$$

$$\phi(t) = \tan^{-1} \left[ \frac{x_s(t)}{x_c(t)} \right] \quad (4-21b)$$

Where  $A(t) \geq 0$  and  $\phi(t)$  is limited to the range 0 to  $2\pi$ .

Introducing  $x_{ct}$ ,  $x_{st}$  and  $x_{rt}$  as the random variables referring to the possible values of  $x_c(t)$ ,  $x_s(t)$  and  $x_r(t)$  respectively,  $x_{ct}$  and  $x_{st}$  are the sums of Gaussian random variables with zero means. They are therefore Gaussian with zero means:

$$E(x_{ct}) = 0 = E(x_{st}) \quad (4-22)$$

The mean square of  $x_{ct}$  is:

$$\begin{aligned} E[(x_{ct})^2] &= \sum_{m=1}^{\infty} \sum_{n=1}^{\infty} \left\{ E[x_{cn} x_{cm} \cos(n\omega_o - \omega_c)t \cos(m\omega_o - \omega_c)t] \right. \\ &+ E[x_{cn} x_{sm} \cos(n\omega_o - \omega_c)t \sin(m\omega_o - \omega_c)t] + E[x_{cm} x_{sn} \cos(m\omega_o - \omega_c)t \sin(n\omega_o - \omega_c)t] \\ &\left. + E[x_{sn} x_{sm} \sin(n\omega_o - \omega_c)t \sin(m\omega_o - \omega_c)t] \right\} \quad (4-23) \end{aligned}$$

Using the orthogonal properties of sinus and cosinus, equation (4-23) simplifies to:

$$E[(x_{ct})^2] = \sum_{n=1}^{\infty} \frac{E(x_{cn})^2}{2} + \sum_{n=1}^{\infty} \frac{E(x_{sn})^2}{2} \quad (4-24)$$

In the same manner:

$$E[(x_{st})^2] = \sum_{n=1}^{\infty} \frac{E(x_{sn})^2}{2} + \sum_{n=1}^{\infty} \frac{E(x_{cn})^2}{2} \quad (4-25)$$

and upon comparison of (4-24) and (4-25)

$$E[(x_{ct})^2] = E[(x_{st})^2] = \sigma_x^2 \quad (4-26)$$

Using the same technique, it is quite easy to show that the covariance of  $x_{ct}$  and  $x_{st}$  is zero

$$E[x_{ct} x_{st}] = 0 \quad (4-27)$$

The random variables  $x_{ct}$  and  $x_{st}$  are therefore independent random variables with zero means and variance  $\sigma_x^2$ . Their joint probability density function can be obtained as:

$$p(x_{ct}, x_{st}) = p(x_{ct}) p(x_{st}) = \frac{1}{2\pi\sigma_x^2} e^{-\frac{x_{ct}^2 + x_{st}^2}{2\sigma_x^2}} \quad (4-28)$$

Now, the joint probability density function of the envelope and phase random variables can be found from:

$$p(A_t, \phi_t) = p(x_{ct}, x_{st}) |J| \quad (4-29)$$

Where  $J$  is the Jacobian of the transformation from  $x_{ct}$  and  $x_{st}$  to  $A_t$  and  $\phi(t)$  as given by equations (4-20a) and (4-20b)

$$J = V_t \quad (4-30)$$

then:

$$p(A_t, \psi_t) = \frac{A_t}{2\pi\sigma_x^2} e^{-\frac{A_t^2}{2\sigma_x^2}} \quad \text{For } V_t < 0 \text{ and } 0 \leq \psi(t) \leq 2\pi \quad (4-31)$$

0

Otherwise

Integrating (4-31) first with respect to  $A_t$  and then with respect to  $\phi(t)$ ,

$$p(\phi_t) = \int_0^{\infty} p(A_t, \phi_t) dA_t \quad (4-32)$$

and

$$p(A_t) = \int_0^{2\pi} p(A_t, \phi_t) d\phi_t \quad (4-33)$$

yields

$$p(\phi_t) = \begin{cases} \frac{1}{2\pi} & 0 \leq \phi_t < 2\pi \\ 0 & \text{Otherwise} \end{cases} \quad (4-34)$$

$$p(A_t) = \begin{cases} \frac{A_t}{\sigma_x^2} e^{-\frac{A_t^2}{2\sigma_x^2}} & A_t \geq 0 \\ 0 & \text{Otherwise} \end{cases} \quad (4-35)$$

It seems from these investigations that the probability density function of the amplitude of the received signal is Rayleigh distributed, if the process is itself Gaussian. This is in good agreement with the results of the experiment conducted in the tank, since the received signals were found to be of the Rayleigh type. Also experiments conducted by other researchers in this field working in model tanks and in the open ocean resulted in practically the same conclusions.

#### 4-4. Investigations of the Final Result

The result of this work consists of a simple equation:

$$\frac{\sigma_e}{V_{\text{rms}}} = k\sigma_w \quad (4-36)$$

Where  $\sigma_e$  is the standard derivation of the envelope of the received signal,  $V_{\text{rms}}$  is the root mean square value of the signal,  $\sigma_w$  is the standard deviation of the waveheights, and  $k$  is a constant of proportionality dependent upon beam pattern, frequency, transducer depth, etc. A direct analytical

derivation of this equation is under attack at the present time and initial results are most promising<sup>10,11</sup>. However, it is possible to develop a logical argument that will give some insight into this equation.

The distortion of a signal can be considered as the ratio of a measure of the signal variation to a measure of the signal strength. The left hand side of equation (4-36) is such a distortion measure in that it is the ratio of the rms value of the envelope (distortion signal) to the rms value of the signal. It is reasonable to expect that this distortion will increase with waveheight since the phase differences between the received rays will increase and become less correlated over the range 0 to  $2\pi$ . The interesting result of this experimental investigation is that this distortion measure varies linearly with average waveheight.

Looked at from another point of view, a horizontal facet is a portion of the water surface with a zero slope near its center and with a small variation in height relative to an acoustic wave length. The power at the receiver is determined by the signal strengths from these facets and will change as their net size changes. The size of the facets in turn depends on the roughness of the surface with the total horizontal area in a sonified area inversely proportional to the roughness<sup>21</sup>. Thus as the roughness of the surface increases, the average received signal power will decrease and the rms value of the envelope tends to decrease because of the decrease in average power while it also tends to increase with the increase phase variation. The ratio of the envelope "power" to the signal power seems to limit these variations to the single variation due to roughness.

## CONCLUSION

The main objective of this report is the observation of sea-state using the reflection of an underwater acoustic signal. Based upon previous work which demonstrated that model tank experiments can be used to arrive at conclusions valid in the ocean, a model tank is used to observe underwater acoustic scattering from a random water surface for different surfaces.

The probability density functions derived theoretically are in agreement with those obtained in the experiment. The probability density functions for the waveheight are approximately Gaussian which compares well with results of other researchers in this area. The probability density functions for the envelope of the received acoustic signal are well approximated by the Rayleigh as found in the literature.

The most significant result was the experimentally derived relationship:

$$\frac{\sigma_e}{V_{\text{rms}}} = k\sigma_w \quad (5-1)$$

which states that the ratio of the envelope variance to the received signal power is directly proportional to the rms waveheight. Although this relationship as yet does not have theoretical verification, intuitive arguments are presented that give credulance to the general form of the equation.

Equation (5-1) suggests that a sea-state indicator can be constructed using a bottom mounted hydrophone. To complete the indicator system, it would only be necessary to devise a circuit to determine the ratio of the rms value of the two signals.

This work suggests the following questions as desirable of additional study:

- 1 - Since only a narrow beamwidth transducer has been used, what is the effect of using wider beamwidth transducer?
- 2 - Could other than normal incidence be used and a Doppler frequency shift observed to measure wave velocity?
- 3 - What is an optimum acoustic frequency for different sea states?
- 4 - Can a more complete statistical analysis be utilized to observe "roughness parameters" as well as average waveheight?
- 5 - What is the effect of white-caps and bubbles near the surface in the real ocean?

## BIBLIOGRAPHY

1. Beckerle, F. C. "Effects of Ocean Waves on Acoustic Signals to Very Deep Hydrophones" Bell Telephone System Technical Publications, Monograph 4487.
2. Cornish, V. "Ocean Waves and Kindred Geophysical Phenomena," (1934).
3. Cox, C. and Munk, W. "Measurements of the Roughness of the Sea Surface from Photographs of the Sun's Glitter," The Journal of the Optical Society of America, Vol. 44, pp. 838-850, 1954.
4. D'Antonio, R. and Hill, R. F. "Communication Characteristics of an Underwater Acoustic Signal Reflected from a Space and Time Random Surface" University of Rhode Island Underwater Acoustics Technical Report No. 7, November, 1964.
5. Davenport, W. B., Jr., and Root, W. L. "An Introduction to the Theory of Random Signals and Noise" McGraw-Hill Book, 1958.
6. Eckart, C. "Scattering of Sound from the Sea Surface" The Journal of the Acoustical Society of America, Vol. 25, No. 3, May, 1953.
7. Gulin, E. P. and Malyshev, K. I. "Statistical Characteristics of Sound Signals Reflected from the Undulating Sea Surface" Soviet-Physics-Acoustics, Vol. 8, No. 3, January-March, 1963.
8. LaCasce, E. O., Jr. "Note on Backscattering of Sound from the Sea Surface" The Journal of the Acoustical Society of America, Vol. 30, No. 6, June 1958.
9. LaCasce, E. O., Jr. and Tamarkin, P. "Underwater Sound Reflection from a Corrugated Surface" Journal of Applied Physics, Vol. 27, No. 2, February 1956.
10. LeBlanc, L., and Hill, R. F. "Measurement and Analysis of Underwater Acoustic Backscattering from a Model Ocean Surface" Presented at the 68th Meeting of The Acoustical Society of America, Austin, Texas, October, 1964.
11. LeBlanc, L. and Hill, R. F. "Analysis of Underwater Acoustic Backscattering from a Random Surface" Presented at the 69th Meeting of The Acoustical Society of America, Washington, D. C., June, 1965.
12. Liebermann, L. N. "Reflection of Underwater Sound from the Sea Surface" The Journal of the Acoustical Society of America, Vol. 20, No. 4, July, 1948.
13. Longuet-Higgins, M. S. "On the Statistical Distribution of the Heights of Sea Waves" Journal of Marine Research, Vol. 11, No.3, 1952.
14. Longuet-Higgins, M. S. "Statistical Properties of an Isotropic Random Surface" Royal Society of London Philosophical Transactions" Series A, Vol. 250, 1957-1958.

15. Munk W. H. "Waves of the Sea" Encyclopedia Brittanica, Vol. 23, pp. 442A-444, 1964.
16. Pierson, W. J., Jr., Newmann, G., and James, R. W. "Practical Methods for Observing and Forecasting Ocean Waves" College of Engineering, New York University, Res. Div., 1953.
17. Richter, R.M. "Measurements of Backscattering from the Sea Surface" The Journal of the Acoustical Society of America, Vol. 36, No. 5, May, 1964.
18. Sverdrup, H. U., Johnson, M. W., and Fleming, R. H. "The Oceans: Their Physics, Chemistry, and General Biology" 1946.
19. Tetreault, D. and Hill, R. F. "Statistical Study of the Wind Driven Surface of an Underwater Acoustic Model Tank" Presented at the 67th Meeting of the Acoustical Society of America, New York City, New York, May, 1964.
20. Whitmarsh, D. C., Skudrzyck, E., and Urlick, R. J. "Forward Scattering of Sound in the Sea and its Correlation with the Temperature Micro-structure" The Journal of the Acoustical Society of America, Vol. 29, No. 10, pp. 1124-1143, October, 1957.
21. Willems, J. and Hill, R. F. "The Statistical Properties of the Slope of a Wind Driven Surface of a Model Tank" Underwater Acoustics Technical Report No. 10, University of Rhode Island, May, 1965.

## DOCUMENT CONTROL DATA - R&amp;D

(Security classification of title, body of abstract and indexing annotation must be entered when the overall report is classified)

1. ORIGINATING ACTIVITY (Corporate author)		2a. REPORT SECURITY CLASSIFICATION	
University of Rhode Island		Unclassified	
		2b. GROUP	
3. REPORT TITLE			
Sea-State Observations with an Underwater Acoustic Signal			
4. DESCRIPTIVE NOTES (Type of report and inclusive dates)			
5. AUTHOR(S) (Last name, first name, initial)			
Jacotin, Leonidas O. Hill, Richard F.			
6. REPORT DATE	7a. TOTAL NO. OF PAGES	7b. NO. OF REFS	
June 15, 1965	37	21	
8a. CONTRACT OR GRANT NO.	9a. ORIGINATOR'S REPORT NUMBER(S)		
N 140(122)76682B	No. 11		
b. PROJECT NO. 42145	9b. OTHER REPORT NO(S) (Any other numbers that may be assigned this report)		
c. 0741807			
d.			
10. AVAILABILITY/LIMITATION NOTICES			
11. SUPPLEMENTARY NOTES		12. SPONSORING MILITARY ACTIVITY	
		U.S. Naval Underwater Ordnance Station Newport, R. I.	
13. ABSTRACT			
<p>This report relates the parameters of the reflected signal to the parameters of the waveheight of the surface of the water. An experiment was conducted simultaneously recording the reflected acoustic signal and the output of a waveheight detector and analyzing each. The experiment states that the received signals are well approximated by a Rayleigh probability density function. The output of the waveheight indicator are Gaussian distributed with increasing maximum amplitude as the wind speed decreases. A linear relationship between the ratio of standard deviation to root mean square value of the signal, and the standard deviation of the waveheights is obtained.</p>			

14. KEY WORDS	LINK A		LINK B		LINK C	
	ROLE	WT	ROLE	WT	ROLE	WT
reflected acoustic signals, sea state, standard deviation, underwater acoustics						

INSTRUCTIONS

1. **ORIGINATING ACTIVITY:** Enter the name and address of the contractor, subcontractor, grantee, Department of Defense activity or other organization (*corporate author*) issuing the report.
- 2a. **REPORT SECURITY CLASSIFICATION:** Enter the overall security classification of the report. Indicate whether "Restricted Data" is included. Marking is to be in accordance with appropriate security regulations.
- 2b. **GROUP:** Automatic downgrading is specified in DoD Directive 5200.10 and Armed Forces Industrial Manual. Enter the group number. Also, when applicable, show that optional markings have been used for Group 3 and Group 4 as authorized.
3. **REPORT TITLE:** Enter the complete report title in all capital letters. Titles in all cases should be unclassified. If a meaningful title cannot be selected without classification, show title classification in all capitals in parenthesis immediately following the title.
4. **DESCRIPTIVE NOTES:** If appropriate, enter the type of report, e.g., interim, progress, summary, annual, or final. Give the inclusive dates when a specific reporting period is covered.
5. **AUTHOR(S):** Enter the name(s) of author(s) as shown on or in the report. Enter last name, first name, middle initial. If military, show rank and branch of service. The name of the principal author is an absolute minimum requirement.
6. **REPORT DATE:** Enter the date of the report as day, month, year; or month, year. If more than one date appears on the report, use date of publication.
- 7a. **TOTAL NUMBER OF PAGES:** The total page count should follow normal pagination procedures, i.e., enter the number of pages containing information.
- 7b. **NUMBER OF REFERENCES:** Enter the total number of references cited in the report.
- 8a. **CONTRACT OR GRANT NUMBER:** If appropriate, enter the applicable number of the contract or grant under which the report was written.
- 8b, 8c, & 8d. **PROJECT NUMBER:** Enter the appropriate military department identification, such as project number, subproject number, system numbers, task number, etc.
- 9a. **ORIGINATOR'S REPORT NUMBER(S):** Enter the official report number by which the document will be identified and controlled by the originating activity. This number must be unique to this report.
- 9b. **OTHER REPORT NUMBER(S):** If the report has been assigned any other report numbers (*either by the originator or by the sponsor*), also enter this number(s).
10. **AVAILABILITY/LIMITATION NOTICES:** Enter any limitations on further dissemination of the report, other than those

imposed by security classification, using standard statements such as:

- (1) "Qualified requesters may obtain copies of this report from DDC."
- (2) "Foreign announcement and dissemination of this report by DDC is not authorized."
- (3) "U. S. Government agencies may obtain copies of this report directly from DDC. Other qualified DDC users shall request through \_\_\_\_\_."
- (4) "U. S. military agencies may obtain copies of this report directly from DDC. Other qualified users shall request through \_\_\_\_\_."
- (5) "All distribution of this report is controlled. Qualified DDC users shall request through \_\_\_\_\_."

If the report has been furnished to the Office of Technical Services, Department of Commerce, for sale to the public, indicate this fact and enter the price, if known.

11. **SUPPLEMENTARY NOTES:** Use for additional explanatory notes.
12. **SPONSORING MILITARY ACTIVITY:** Enter the name of the departmental project office or laboratory sponsoring (*paying for*) the research and development. Include address.
13. **ABSTRACT:** Enter an abstract giving a brief and factual summary of the document indicative of the report, even though it may also appear elsewhere in the body of the technical report. If additional space is required, a continuation sheet shall be attached.  
It is highly desirable that the abstract of classified reports be unclassified. Each paragraph of the abstract shall end with an indication of the military security classification of the information in the paragraph, represented as (TS), (S), (C), or (U).  
There is no limitation on the length of the abstract. However, the suggested length is from 150 to 225 words.
14. **KEY WORDS:** Key words are technically meaningful terms or short phrases that characterize a report and may be used as index entries for cataloging the report. Key words must be selected so that no security classification is required. Identifiers, such as equipment model designation, trade name, military project code name, geographic location, may be used as key words but will be followed by an indication of technical context. The assignment of links, roles, and weights is optional.